Published in final edited form as:
J Immunol. 2013 July 1; 191(1): 110–116. doi:10.4049/jimmunol.1202849.

Ro60 Requires Y3 RNA for Cell Surface Exposure and Inflammation Associated with Cardiac Manifestations of Neonatal Lupus

Joanne H. Reed[*], **Soyeong Sim**[†], **Sandra L. Wolin**[†], **Robert M. Clancy**[*], and **Jill P. Buyon**[*]

[*]Department of Medicine, New York University School of Medicine, 560 First Avenue, New York, NY 10016, USA

[†]Department of Cell Biology, Yale University School of Medicine, 295 Congress Avenue, New Haven, CT 06536, USA

Abstract

Cardiac neonatal lupus (NL) is presumed to arise from maternal autoantibody targeting an intracellular ribonucleoprotein, Ro60, which binds noncoding Y RNA and only becomes accessible to autoantibodies during apoptosis. Despite the importance of Ro60 trafficking in the development of cardiac-NL, the mechanism underlying cell surface exposure is unknown. To evaluate the influence of Y RNA on the subcellular location of Ro60 during apoptosis and activation of macrophages, stable Ro60 knockout murine fibroblasts expressing wild-type or mutated FLAG-Ro60 were assessed. $FLAG_3$-Ro60(K170A R174A) binds Y RNA, whereas $FLAG_3$-Ro60(H187S) does not bind Y RNA; fibroblasts expressing these constructs showed equivalent intracellular expression of Ro60. In contrast, apoptotic fibroblasts containing $FLAG_3$-Ro60(K170A R174A) were bound by anti-Ro60, whereas $FLAG_3$-Ro60(H187S) was not surface expressed. RNA interference of mY3 RNA in wild-type fibroblasts inhibited surface translocation of Ro60 during apoptosis, while depletion of mY1 RNA did not affect Ro60 exposure. Furthermore, Ro60 was not exposed following overexpression of mY1 in the mY3 depleted fibroblasts. In an in vitro model of anti-Ro60-mediated injury, Y RNA was shown to be an obligate factor for TLR-dependent activation of macrophages challenged with anti-Ro60-opsonized apoptotic fibroblasts. Murine Y3 RNA is a necessary factor to support the surface translocation of Ro60, which is pivotal to the formation of immune complexes on apoptotic cells and a TLR-dependent proinflammatory cascade. Accordingly, the Y3 RNA moiety of the Ro60 ribonucleoprotein imparts a critical role in the pathogenicity of maternal anti-Ro60 autoantibodies.

Introduction

Cardiac manifestations of neonatal lupus (cardiac-NL), which comprise complete atrioventricular block but in some cases more extensive injury such as cardiomyopathy, result in fetal death in a fifth of cases and lifelong pacemaker implantation in most surviving infants (1). Cardiac injury occurs in a previously normal fetus and is presumed to arise from the transplacental passage of maternal autoantibodies (Abs) targeting the intracellular antigens 60kD Ro/SSA, 52kD Ro/SSA, and 48kD La/SSB (2). Apoptosis has been posited as a means by which these normally inaccessible antigens can be trafficked to the cell membrane and bound by extracellular Abs to initiate injury (3–5). The translocation of Ro and La to apoptotic membrane blebs was first demonstrated in cultured human keratinocytes

Address for correspondence and reprints: Joanne H. Reed, Ph.D. New York University School of Medicine, Department of Medicine, Division of Rheumatology, 560 First Avenue, New York, NY 10016, Phone 212-263-2676, Fax 212-263-0759, joanne.reed@nyumc.org.

(3) and subsequently in human fetal cardiomyocytes. Moreover binding of maternal Abs was shown to inhibit uptake by healthy cardiomyocytes (5, 6). Further insights into cardiac injury were provided by histological studies of hearts from several fetuses dying with cardiac-NL revealing clusters of macrophages colocalized with apoptotic cells and IgG and enhanced expression of proinflammatory and profibrotic factors compared to healthy fetal hearts (7). Based on these in vitro and in vivo findings, we postulate that the binding of maternal anti-Ro/La Abs to translocated antigens converts the physiologic process of apoptosis, which occurs during fetal development, into one in which an inflammatory component is evoked. This inflammatory component may be due to the RNA binding properties of the 60kD Ro (Ro60) antigen.

Crystallographic studies of Ro60 have revealed a ring-shaped protein with two overlapping RNA binding sites and provided new insights into function which may vary depending on subcellular location (8). In the nucleus, misfolded RNA binds the central cavity and basic surface of the Ro ring, raising the possibility that Ro60 plays a role in RNA quality control (9, 10). In the cytoplasm, Ro60 binds a class of noncoding RNA termed Y RNA, on the outer surface of the ring. La also associates with Y RNAs however, this interaction is transient and occurs in the nucleus following transcription (11, 12). The function of Y RNAs is related to Ro60 as these transcripts are unstable in Ro60 deficient cells (13, 14). Y RNAs have been shown to modulate the function of Ro60 by masking the Ro central cavity binding site to other RNAs (15), altering the subcellular location of Ro60 (16), and forming complexes with other proteins (17, 18). The cytoplasmic localization of Ro60 appears to be dependent on the presence of Y RNA since a mutated Ro60 that is unable to bind Y RNA accumulates in nuclei (16). Ro60 also accumulates in nuclei when Y RNAs are depleted using siRNAs (16). These observations are consistent with a model in which Y RNA masks a nuclear localization signal on Ro60, thereby retaining the protein in the cytoplasm. While it is unknown whether Y RNA plays a role in the cell surface translocation of Ro60, it is likely that this RNA moiety contributes to anti-Ro60 Ab-mediated tissue injury as immune complexes composed of Ro60, Y RNA and anti-Ro60 Ab promote TLR7-dependent TNFα secretion from macrophages (19).

Despite the relevance of Ro60 translocation to the initiation of tissue injury in cardiac-NL, the mechanisms underlying cell surface exposure during apoptosis are unknown. Given the potential for Y RNA to modulate the subcellular location of Ro60 and initiate inflammatory responses in macrophages, the current study explores the requirement of Y RNA for Ro60 translocation and subsequent activation of TLR signaling. Cells expressing Ro60 mutants in which single amino acid substitutions influence the binding of associated RNA were used, together with RNA interference and overexpression of specific Y RNA subsets, to address the dependency of Y RNA in the translocation of Ro60 during apoptosis.

Materials and Methods

Autoantibodies

Affinity purified anti-Ro60 or anti-La Abs were isolated from the serum of a mother with a child with cardiac-NL (n=5 anti-Ro60, n=3 anti-La) by affinity column chromatography using recombinant Ro60 or La coupled to Affigel10 (BioRad) as previously described (6). Eluted Abs were tested for specificity by ELISA and immunoblot (4, 6). All mothers were enrolled in the Research Registry for Neonatal Lupus and signed informed consent approved by the New York University School of Medicine Institutional Review Board for the use of their sera. Control IgG was isolated from the sera of healthy adults (n=3) using a Protein A-IgG isolation kit (Pierce, Rockford, IL) according to manufacturer's recommendations. IgG fractions were treated with Detoxi-Gel™ Endotoxin Removing Gel and lipopolysaccharide

concentration was <1 EU/ml as assessed by the Limulus Amebocyte Lysate Endotoxin Quantification Assay (Lonza).

Cells

The wild-type and Ro60 knockout murine fibroblasts have been described (16), as has the generation of stable Ro60 knockout fibroblast lines expressing wild-type $FLAG_3$-Ro, and $FLAG_3$-Ro60 containing either the single point mutation H187S or the two point mutations K170A and R174A (16). The H187S point mutation does not stably bind Y RNA, whereas K170A R174A mutations do not affect the Ro60 Y RNA interaction. All fibroblasts were cultured in DMEM (Invitrogen) containing 10% FBS and 2 mmol/L L-glutamine. Human macrophages derived from PBMCs were obtained from random healthy donors (New York Blood Center, New York, NY) by centrifugation on Ficoll-Hypaque gradients and positive selection using anti-CD14 microbeads (Miltenyi Biotech). Isolated CD14-positive cells were cultured in Teflon beakers (RPMI 1640/10% FBS) for 7 days in the presence of GM-CSF (19, 20). The human monocytic cell line, THP-1 was obtained from the ATCC and cultured in RPMI 1640 with 10% FBS. THP-1 cells were differentiated with 0.2 μmol/L phorbol myristate acetate (PMA) for 3 days followed by 48 hours in RPMI/10% FBS without PMA as described (21).

Knockdown of mY1 and mY3 RNAs and northern blot

Small interfering (si) RNA targeting mY1 or mY3 were designed as described (16). NonTargeting siRNA 1 (Dharmacon, Lafayette, CO) was used as a control. Wild-type murine fibroblasts (1×10^6) in growth medium were transfected with 400 pmol siRNA mixed with 37.5 μl Lipofectamine 2000 (Invitrogen) in $75cm^2$ flasks. After 48 hours, cells were harvested in HBSS (Invitrogen). To confirm knockdown, RNA was prepared from ~2×10^5 cells and subjected to northern blot with oligonucleotide probes to detect mY1, mY3 RNA and 5S rRNA as described (16). Y RNA expression was calculated by the following equation: quantification of pixels for mY1 or mY3 immunoblot/quantification of pixels for 5S rRNA) x100. Y RNA levels were presented as a ratio of expression relative to untreated cells. The siRNA-treated cells were permeabilized or rendered apoptotic to evaluate intracellular or extracellular expression of Ro60, respectively as described below.

Overexpression of mY1 and mY3 RNAs

To overexpress Y RNAs, the genes and flanking regions were amplified from mouse genomic DNA and cloned into the EcoRI and BamHI sites of pBluescriptII KS+. The mY3 clone has 484 nt of upstream and 225 nt of downstream sequence, while the mY1 clone has 527 nt of upstream and 248 nt of downstream sequence. Wild-type fibroblasts in growth medium were co-transfected using Lipofectamine 2000 with 1 μg plasmid and 400 pmol siRNA. After 48 hours, cells were harvested in HBSS and Y RNA overexpression and/or knockdown was confirmed by northern blotting (16). Intracellular and extracellular expression of Ro60 was evaluated as described below.

Induction of apoptosis in murine fibroblasts

Apoptosis was induced by treating fibroblasts with 0.1 μg/ml murine interferon (IFN)-γ for 24 hr. Cells were then seeded onto tissue culture dishes coated with poly(2-hydroxyethyl methacrylate) which disrupts adhesion to the surface and hence stimulatory signals received during growth in the presence of IFN-γ (0.1 μg/ml), TNFα (5 ng/ml), and cycloheximide (100 μg/ml) for 4 to 18 hr (5). Apoptosis was confirmed by flow cytometric analysis of phosphatidylserine exposure (annexin V binding). The integrity of apoptotic cell membrane was monitored by propidium iodide (PI).

Flow cytometry for evaluation of Ro60 expression

Intracellular expression of Ro60 was evaluated on cultured fibroblasts using the BD Cytofix/Cytoperm™ kit (BD Biosciences) according to manufacturer's recommendations. Extracellular expression of Ro60 was assessed on non-fixed, non-permeable, early apoptotic fibroblasts gated as annexin V-positive, PI-negative. Cells (permeabilized or apoptotic) were incubated with 5 μg/ml affinity purified Abs for 45 minutes at room temperature. After incubation cells were washed twice (PBS/1% BSA/0.02% sodium azide) and stained with anti-human IgG-FITC (1/200) for 30 min. For apoptotic cells, 5 μl annexin V-APC (BD Biosciences) and 5 μg/ml PI (Invitrogen) in annexin V binding buffer (10 mmol/L HEPES, 140 mmol/L NaCl, 2.5 mmol/L $CaCl_2$ pH 7.4) were added for 15 minutes at room temperature. Binding was assessed on a LSRII flow cytometer (BD Biosciences).

Evaluating intracellular Ro60 expression by immunoblot

Fibroblasts were lysed in Tris-buffered saline containing 1% Nonidet P-40 and protease inhibitors (Roche) for 30 min on ice. Lysates were subjected to SDS-PAGE, transferred to PVDF membranes and blocked with 5% nonfat skim milk powder in PBS overnight at 4°C. After three washes (PBS/0.1% Tween 20), membranes were probed with either human anti-Ro60 Ab (1 μg/ml) or anti-FLAG mAb (0.5 μg/ml) for 1 hour at room temperature. Membranes were stained with IRDye 800CW anti-human or anti-mouse IgG conjugates and analyzed on the Odyssey Infrared Imager (LI-COR Biosciences).

Co-cultures of apoptotic fibroblasts and macrophages

For co-culture experiments PBMC-derived macrophages or PMA-differentiated THP-1 cells (2×10^5 per well) were seeded in 24-well tissue culture plates. After washing twice with HBSS, cells were primed with 50 pg/ml IFN-γ in serum free RPMI for 6 hours. Apoptotic murine fibroblasts incubated with control IgG or anti-Ro60 Ab for 45 min at room temperature were then washed twice and added to IFN-γ primed macrophages or THP-1 cells for 18 hours. To confirm dependence on TLR7 signaling, 10 μg/ml of the TLR7 inhibitor (IRS661 (22), a generous gift from Dr. Franck Barrat, Dynavax Technologies, Berkeley, CA) was added to macrophages 30 min prior to the addition of apoptotic fibroblasts. In other experiments, the protective properties of the plasma protein β_2GPI, previously shown to compete with anti-Ro60 Ab for binding to apoptotic cells, were evaluated. β_2GPI (1–50 μg/ml) was co-incubated with anti-Ro60 Ab and apoptotic fibroblasts prior to the addition to macrophages. Conditioned media from the culturing conditions was centrifuged at 14,000 rpm for 3 min to remove cell debris. The readout of TLR signaling was the release of the inflammatory cytokine, TNFα measured by ELISA (R&D Systems) according to manufacturer's instructions.

Statistical analysis

For flow cytometry experiments, the binding of affinity purified Ab was expressed as the mean fluorescence intensity (MFI) minus the baseline MFI of cells treated with secondary antibody only. Anti-Ro60 binding was normalized by dividing the MFI of siRNA treated fibroblasts by the MFI of untreated fibroblasts x100. The percent inhibition of TNFα secretion was evaluated by dividing the TNFα concentration in the presence of IRS661 or β_2GPI by the TNFα concentration in the absence of IRS661 or β_2GPI. Differences were compared by one-way analysis of variance (ANOVA) or repeated measures ANOVA with Bonferroni post-hoc analysis where appropriate. A P-value less than 0.05 was considered statistically significant.

Results

Intracellular expression of Ro60 is equivalent in knockout fibroblasts stably expressing varied $FLAG_3$-Ro60 constructs

As our experimental system, we used murine Ro60 knockout fibroblasts that stably express epitope-tagged wild-type Ro60 ($FLAG_3$-Ro60) and two mutant forms of Ro60, $FLAG_3$-Ro60(H187S) and $FLAG_3$-Ro60(K170A R174A), as their only form of Ro60. Previous characterization of these cell lines demonstrated that although Y RNAs are reduced ~30-fold in the Ro60 knockout fibroblasts and $FLAG_3$-Ro60(H187S) cells (16, 23), these RNAs are present at near wild-type levels in the $FLAG_3$-Ro60 and $FLAG_3$-Ro60(K170A R174A) cells (16). Initial experiments were done to assure intracellular binding of human affinity purified anti-Ro60 Ab to murine wild-type and mutated Ro60 and to compare intracellular levels of Ro60 across the different fibroblast cell lines. Permeabilized wild-type murine fibroblasts were bound by human anti-Ro60 but not control IgG (MFI 4,614 ±413 vs. 145±60, $P<0.0005$), substantiating cross-reactivity between murine Ro60 and human anti-Ro60 Ab. The specificity of the anti-Ro60 Ab was confirmed by the absence of binding to permeabilized Ro60 knockout fibroblasts (MFI 33±33). Despite differences in Y RNA content, both $FLAG_3$-Ro60(K170A R174A) and $FLAG_3$-Ro60(H187S) cells showed equivalent intracellular binding of anti-Ro60 (MFI 1,664±355 and 1,471±699, P-value not significant (NS)). In cells stably expressing wild-type $FLAG_3$-Ro60, intracellular expression of Ro60 was similar to that observed with $FLAG_3$-Ro60(K170A R174A) and $FLAG_3$-Ro60(H187S) mutant cells (MFI 2,280 ±539, P=NS). None of the permeabilized fibroblast cell lines bound control IgG (Figure 1A). Intracellular expression of Ro60 was also compared among fibroblasts expressing $FLAG_3$-Ro60 constructs by evaluating binding of anti-FLAG mAb after permeabilization. Fibroblasts expressing $FLAG_3$-Ro60, $FLAG_3$-Ro60(K170A R174A) and $FLAG_3$-Ro60(H187S) showed equivalent reactivity with anti-FLAG mAb (MFI 1,800 ±158, 1,886 ±156, and 1,681 ±38 respectively, P-value NS for all comparisons). As expected, wild-type and Ro60 knockout fibroblasts did not react with anti-FLAG mAb (MFI 19 ±11 and 6 ±3, respectively) (Figure 1B). Ro60 and FLAG expression was confirmed by immunoblot with human anti-Ro60 Ab or anti-FLAG mAb (Figure 1C). Intracellular expression of La, an autoantigen that also interacts with Y RNA, was evaluated on the murine fibroblast lines to determine whether Ro60/Y RNA composition (or absence) affects La expression. Affinity purified anti-La Ab showed equivalent binding to all murine fibroblasts independent of the expression of Ro60/Y RNA (Figure 1D).

Surface translocation of Ro60 during apoptosis varies in fibroblasts expressing mutated $FLAG_3$-Ro60 constructs

Having established equivalent intracellular expression of Ro60 in fibroblasts expressing $FLAG_3$ constructs, cell surface expression of Ro60 was then evaluated. Murine fibroblasts were rendered apoptotic and binding of anti-Ro60 Ab was measured by flow cytometry. Apoptotic cells were gated according to annexin V and PI-staining where early apoptotic cells were annexin V-positive and PI-negative (i.e. maintained membrane integrity). Late apoptotic cells were both annexin V and PI-positive (Figure 2A). Early apoptotic fibroblasts expressing $FLAG_3$-Ro60(K170A R174A) (binds Y RNA) were bound by anti-Ro60 Ab but not control IgG (MFI 254 ±79 vs. 27±15, $P<0.05$). While cell surface expression of this Ro60 mutant was significantly less than wild-type murine fibroblasts (MFI 659±74, $P<0.05$ vs. $FLAG_3$-Ro60(K170A R174A)), expression was equivalent to wild-type $FLAG_3$-Ro60 (MFI 274±92, P=NS vs. $FLAG_3$-Ro60(K170A R174A)). In contrast, apoptotic fibroblasts expressing $FLAG_3$-Ro60(H187S) were not bound by anti-Ro60 Ab (MFI 30±20 vs. $FLAG_3$-Ro60(K170A R174A), $P<0.05$, vs. wild-type, $P<0.0005$, vs. $FLAG_3$-Ro60, $P<0.05$) and showed an equivalent MFI to Ro60 knockout apoptotic cells (MFI 19±17, P=NS, vs $FLAG_3$-Ro60(H187S)) and that obtained when incubating with control IgG (Figure 2B).

Late apoptotic fibroblasts showed similar binding profiles as early apoptotic for each fibroblast line (wild-type: MFI 1,824±531; knockout: MFI 53±35; $FLAG_3$-Ro60: MFI 795±243; $FLAG_3$-Ro60(K170A R174A): MFI 873±292; $FLAG_3$-Ro60(H187S): MFI 178±30) (Figure 2C). La, previously shown to be expressed on late apoptotic cells (24), was also evaluated on apoptotic murine fibroblasts to determine whether translocation of this autoantigen required Ro60 or Y RNA. Affinity purified anti-La Ab showed equivalent binding to late apoptotic fibroblasts regardless of Ro60/Y RNA expression (Figure 2D).

Cell surface translocation of Ro60 during apoptosis is dependent on mY3 RNA

Since the Ro60 mutations $FLAG_3$-Ro60(K170A R174A) and $FLAG_3$-Ro60(H187S) differ in their ability to bind Y RNA, it was hypothesized that the absence of Y RNA bound to $FLAG_3$-Ro60(H187S) accounts for the reduced expression of this mutant Ro60 on the surface of apoptotic cells. To test whether Y RNA is a requirement for translocation of Ro60 to the cell surface, both murine Y RNA subsets, mY1 and mY3, were depleted in wild-type fibroblasts and surface expression of Ro60 was evaluated. Northern blot revealed that RNA interference depleted the appropriate mY1 or mY3 RNA from wild-type fibroblasts while 5S rRNA, used as a loading control, was not altered by siRNA transfection (Figure 3A,C). To determine whether intracellular expression of Ro60 was affected by the depletion of Y RNA, anti-Ro60 binding to permeabilized cells was evaluated by flow cytometry. Intracellular Ro60 levels were comparable among wild-type fibroblasts transfected with control (98±7%), mY1 (95±10%), mY3 (93±10%), or both mY1/mY3 (94±8%) siRNA where the binding of anti-Ro60 Ab to untreated fibroblasts is 100%. In contrast, when siRNA transfected fibroblasts were rendered apoptotic, translocation of Ro60 was significantly reduced in fibroblasts depleted of mY3 RNA compared to control siRNA treated cells (12±7 vs. 101±25% respectively, $P<0.005$). However, depletion of mY1 RNA from wild-type fibroblasts did not affect the translocation of Ro60 (102±25%, P=NS vs. control siRNA, $P<0.005$ vs. mY3 siRNA treated cells). The simultaneous depletion of mY1 and mY3 RNA from wild-type fibroblasts impaired the translocation of Ro60 (4±3%) to the same extent as that of mY3 RNA depletion alone (P=NS vs. mY3 siRNA treated cells) (Figure 3E).

If mY3 is more abundant than mY1, knockdown of mY1 may have a negligible effect on Ro60/Y RNA complexes since the remaining mY3 RNA may be sufficient to sequester Ro60 in the cytoplasm. However, in wild-type fibroblasts co-transfected with mY1 plasmids and mY3 siRNA to simultaneously overexpress mY1 while depleting mY3, anti-Ro60 binding to the surface of apoptotic fibroblasts was similar to that observed when the cells were treated with mY3 siRNA alone (Figure 3F). Northern blotting confirmed that wild-type fibroblasts transfected with mY1 plasmids overexpressed mY1 RNA relative to untreated cells (Figure 3B,D). Interestingly, overexpression of mY1 was associated with decreased levels of mY3, suggesting that mY1 and mY3 RNAs compete for binding to Ro60. Consistent with competition for Ro60 binding, the overexpression of mY1 RNA was further increased when mY3 siRNA was co-transfected with mY1 plasmids compared to control siRNA (Figure 3B, D). However, while Ro60 required mY3 RNA for surface translocation, the levels of mY3 did not influence the amount of surface expressed Ro60, indicating that the lower levels of mY3 remaining after mY1 overexpression were adequate for Ro60 surface translocation. Moreover, overexpression of mY3 RNA (by approximately 2-fold) did not enhance anti-Ro60 binding to apoptotic fibroblasts relative to untreated apoptotic fibroblasts (Figure 3F).

Apoptotic fibroblast immune complexes containing Y RNA stimulate TLR7-dependent TNFα secretion by Macrophages

Given the varied expression of the mutated forms of Ro60 on the surface of apoptotic cells and the requirement of Y RNA for Ro60 translocation, the functional consequences of surface bound Ro60/Y RNA-anti-Ro60 complexes were subsequently addressed in co-culture experiments. Human PBMC-derived macrophages cultured with apoptotic fibroblasts expressing $FLAG_3$-Ro60(K170A R174A) preincubated with anti-Ro60, secreted significantly higher levels of TNFα compared to macrophages incubated with $FLAG_3$-Ro60(H187S) apoptotic fibroblasts similarly preincubated with anti-Ro60 (85±27 pg/ml vs. 34±2 pg/ml respectively, $P<0.05$). Macrophages co-cultured with wild-type and $FLAG_3$-Ro60 apoptotic fibroblasts bound by anti-Ro60 Ab showed similar TNFα readouts compared to $FLAG_3$-Ro60(K170A R174A) apoptotic fibroblasts (wild-type: 109±24 pg/ml and $FLAG_3$-Ro60: 106±25 pg/ml, P=NS for all comparisons. In contrast, macrophages cultured with Ro60 knockout apoptotic fibroblasts preincubated with anti-Ro60 showed reduced levels of TNFα (22±5 pg/ml). Preincubation of apoptotic fibroblasts with control IgG prior to culturing with macrophages did not enhance TNFα secretion (Figure 4A). Co-culture experiments with PMA-differentiated THP-1 cells showed a similar pattern of TNFα secretion as human macrophages (Figure 4B). Treatment of THP-1 cells with anti-Ro60 opsonized apoptotic wild-type fibroblasts stimulated TNFα release compared to challenge with Ro60 knockout fibroblasts preincubated with anti-Ro60 (85 ±26 vs. 25±2, $P<0.05$), an effect also observed with challenge using $FLAG_3$-Ro60(K170A R174A) but not $FLAG_3$-Ro60(H187S) (80±13 vs 43±12 pg/ml (Figure 4B). TNFα secretion by THP-1 cells co-cultured with wild-type, $FLAG_3$-Ro60, or $FLAG_3$-Ro60(K170A R174A) apoptotic fibroblasts, all opsonized with anti-Ro60 Ab, was inhibited by 43±6% ($P<0.005$), 43±7% ($P<0.05$), and 47±3% ($P<0.005$) respectively in the presence of the TLR7 inhibitor, IRS661 (Figure 4C). To further evaluate the requirement of Ro60 accessibility to Ab for TLR-mediated inflammation we determined whether blocking Ro60 on apoptotic cells would reduce TNFα secretion in co-culture experiments. Plasma protein, beta2-glycoprotein I (β_2GPI), previously shown to bind Ro60 on the surface of apoptotic cells and block the binding of anti-Ro60 Ab (25, 26), was added to apoptotic wild-type fibroblasts prior to anti-Ro60 Ab. The fibroblasts were then cultured with PMA-differentiated THP-1 cells. Human native β_2GPI bound late apoptotic fibroblasts (data not shown). The addition of β_2GPI to apoptotic fibroblasts prior to anti-Ro60 Ab and co-culturing with THP-1 cells resulted in a dose-dependent inhibition of TNFα secretion (range of inhibition 20–70% with 1–50 μg/ml β_2GPI compared to co-culture experiments without β_2GPI) (Figure 4D).

Discussion

Exaggerated apoptosis has been proposed as a pathologic link between anti-Ro60 Abs and injury in cardiac-NL and provides a mechanism for facilitating accessibility of an otherwise intracellular autoantigen to circulating maternal Abs (5). In order to test the hypothesis that Y RNA is critical for the translocation of Ro60 to the apoptotic cell surface, initial experiments exploited murine fibroblasts stably expressing mutations of Ro60 which affect Y RNA binding. Two experimental approaches supported the dependence of Y RNA for surface translocation of Ro60; absence of anti-Ro60 Ab binding to apoptotic fibroblasts expressing a Ro60 point mutation (H187S) which prevents Y RNA binding and wild-type murine fibroblasts depleted of mY3 RNA. Moreover, the translocation of Ro60 during apoptosis and subsequent opsonization by anti-Ro60 Ab is highlighted as a key mediator for the initiation and perpetuation of inflammation via TLRs as cells expressing $FLAG_3$-Ro60(H187S) do not activate macrophages since this mutated protein is not exposed on the cell surface. In contrast, $FLAG_3$-Ro60(K170A R174A) and $FLAG_3$-Ro60 (both bind Y RNA) translocate to the cell surface during apoptosis and activate macrophages in a TLR-

dependent manner. These results support the hypothesis that Y RNA plays a critical role in the pathogenesis of fetal cardiac injury by altering the subcellular location of Ro60.

Translocation of Ro60 to the apoptotic cell surface was dependent on mY3 RNA but not mY1 RNA as depletion of mY3 prevented cell surface translocation of Ro60 whereas depletion of mY1 had no effect. This finding is consistent with the previous observation that depletion of mY3 RNA in murine astrocytoma cells resulted in nuclear accumulation of Ro60. In contrast, Ro60 was retained in the cytoplasm after mY1 RNA knockdown (16). Initially we postulated that mY1 RNA by being less abundant than mY3 was not sufficient to sequester Ro60 in the cytoplasm (for subsequent transport to the cell surface during apoptosis) in mY3 depleted fibroblasts. However, increased expression of mY1 RNA did not overcome the absence of Ro60 translocation upon mY3 depletion. Several non-mutually exclusive explanations are plausible to account for the differential effects of mY3 and mY1 RNA knockdown. For the latter, retention of a fragment of the 5′ mY1 RNA stem following knockdown may be sufficient to mask the Ro60 nuclear localization signal (16). Another possibility is that cell surface translocation is restricted to Ro60 associated with mY3 RNA, and may explain, in part, why levels of surface exposed Ro60 tend to be lower than intracellular levels. The molecular explanation notwithstanding, the differences observed in Ro60 translocation after mY1 and mY3 depletion would imply distinct roles for the Y RNA subsets, a concept that was previously considered when particular subsets of Y RNAs associated with specific proteins (17, 27). For example, the zipcode binding protein 1 was recently reported to associate with Ro60/mY3 RNA complexes for nuclear export but not Ro60/mY1 RNA complexes (18). It is possible that a protein that interacts exclusively with Ro60/mY3 RNA complexes may chaperone the antigen to the cell surface during apoptosis.

The participation of Y RNA in cellular trafficking appears to be specific to Ro60 as intracellular expression and cell surface exposure of La was not affected in apoptotic cells with significantly reduced levels of Y RNA (Ro60 knockout or $FLAG_3$-Ro60(H187S)). In support of these data, a previous study found that the association of Y RNA with La may be partially lost during apoptosis as immunoprecipitation of apoptotic cell lysates with anti-Ro60 Ab yielded more Y RNA than immunoprecipitation with anti-La Ab (28). Moreover, La predominantly binds Y RNA in the nucleus whereas during apoptosis, La undergoes caspase-dependent cleavage of the COOH-terminal nuclear localization signal and accumulates in the cytoplasm (29). Together these data imply that the mechanism of La translocation during apoptosis is independent of Y RNA.

Perhaps paradoxical to the findings of this study, apoptosis has been demonstrated to induce a caspase-dependent truncation of Y RNAs. However, the resulting 22 to 36 nucleotide degradation products correspond to the most highly conserved region of the Y RNA which remains bound to Ro60 (28). Thus, it is predicted that these truncated products would still mask the Ro60 nuclear localization signal allowing cell surface translocation of cytosolic Ro60/mY3 RNA complexes. The truncated Y RNA remaining after apoptosis should not only facilitate surface translocation but also be sufficient to engage TLRs during macrophage FcγR mediated uptake of anti-Ro60 opsonized apoptotic cells (30).

In summary, a single point mutation of Ro60 which blocks Y RNA binding and siRNA-mediated knockdown of mY3 RNA attenuate a permissive signal that is required for surface accessibility of the Ro60 antigen to bind extracellular Ab and form immune complexes capable of inciting a TLR-dependent proinflammatory cascade. Accordingly, the mY3 RNA moiety of the Ro60 ribonucleoprotein imparts a critical role to the pathogenicity of anti-Ro60 Ab. The molecular dissection of the components involved in the pathogenesis of cardiac-NL including, translocation of Ro60 during apoptosis, Ro60 associated RNA, and

binding of anti-Ro60 Ab to apoptotic cells and potential protective factors such as β_2GPI may lead to novel therapeutic approaches.

Acknowledgments

This work was supported by American Heart Association Postdoctoral Fellowship (to J.H.R), Australian National Health and Medical Research Council Overseas Postdoctoral Research Grant 595989 (to J.H.R), Arthritis Foundation Postdoctoral Fellowship (to J.H.R), NIH Grant R01 GM073863 (to S.L.W.), a grant from the Lupus Research Institute, Inc. (to S.L.W), and NIH Merit Award R37 AR042455 (to J.P.B).

We thank the Flow Cytometry and Cell Sorting Center at the New York University Langone Medical Center for technical assistance with flow cytometry experiments.

Abbreviations used in this article

β_2GPI	beta2-glycoprotein I
MFI	mean fluorescence intensity
NL	neonatal lupus
PI	propidium iodide
siRNA	small interfering RNA

References

1. Buyon, JP.; Friedman, DM. Neonatal Lupus. In: Lahita, RG.; Tsokos, G.; Buyon, JP.; Koike, T., editors. Systemic Lupus Erythematosus. 5. Academic Press; San Diego, CA: 2011. p. 541-567.
2. Buyon JP, Winchester R. Congenital complete heart block: A human model of passively acquired autoimmune injury. Arthritis Rheum. 1990; 33:609–614. [PubMed: 2346516]
3. Casciola-Rosen L, Anhalt G, Rosen A. Autoantigens targeted in systemic lupus erythematosus are clustered in two populations of surface structures on apoptotic keratinocytes. J Exp Med. 1994; 179:1317–1330. [PubMed: 7511686]
4. Miranda-Carus ME, Boutjdir M, Tseng CE, DiDonato F, Chan EK, Buyon JP. Induction of antibodies reactive with SSA/Ro-SSB/La and development of congenital heart block in a murine model. J Immunol. 1998; 161:5886–5892. [PubMed: 9834068]
5. Clancy RM, Neufing PJ, Zheng P, O'Mahony M, Nimmerjahn F, Gordon TP, Buyon JP. Impaired clearance of apoptotic cardiocytes is linked to anti-SSA/Ro and -SSB/La antibodies in the pathogenesis of congenital heart block. J Clin Invest. 2006; 116:2413–2422. [PubMed: 16906225]
6. Miranda-Carus ME, Tseng CE, Rashbaum W, Ochs RL, Casiano CA, Di Donato F, Chan EK, Buyon JP. Accessibility of SSA/Ro and SSB/La antigens to maternal autoantibodies in apoptotic human fetal cardiac myocytes. J Immunol. 1998; 161:5061–5069. [PubMed: 9794444]
7. Clancy RM, Kapur RP, Molad Y, Askanase AD, Buyon JP. Immunohistologic evidence supports apoptosis, IgG deposition, and novel macrophage/fibroblast crosstalk in the pathologic cascade leading to congenital heart block. Arthritis Rheum. 2004; 50:173–182. [PubMed: 14730614]
8. Stein AJ, Fuchs G, Fu C, Wolin SL, Reinisch KM. Structural insights into RNA quality control: the Ro autoantigen binds misfolded RNAs via its central cavity. Cell. 2005; 121:529–539. [PubMed: 15907467]
9. O'Brien CA, Wolin SL. A possible role for the 60 kD Ro autoantigen in a discard pathway for defective 5S ribosomal RNA precursors. Genes Dev. 1994; 8:2891–2903. [PubMed: 7995526]
10. Chen X, Smith JD, Shi H, Yang DD, Flavell RA, Wolin SL. The Ro autoantigen binds misfolded U2 small nuclear RNAs and assists mammalian cell survival after UV irradiation. Curr Biol. 2003; 13:2206–2211. [PubMed: 14680639]
11. Hendrick JP, Wolin SL, Rinke J, Lerner MR, Steitz JA. Ro small cytoplasmic ribonucleoproteins are a subclass of La ribonucleoproteins: further characterization of the Ro and La small

ribonucleoproteins from uninfected mammalian cells. Mol Cell Biol. 1981; 1:1138–1149. [PubMed: 6180298]

12. Simons FH, Pruijn GJ, van Venrooij WJ. Analysis of the intracellular localization and assembly of Ro ribonucleoprotein particles by microinjection into Xenopus laevis oocytes. J Cell Biol. 1994; 125:981–988. [PubMed: 8195301]
13. Labbe JC, Hekimi S, Rokeach LA. The levels of the RoRNP-associated Y RNA are dependent upon the presence of ROP-1, the Caenorhabditis elegans Ro60 protein. Genetics. 1999; 151:143–150. [PubMed: 9872955]
14. Xue D, Shi H, Smith J, Chen X, Noe N, Cedervall T, Yang D, Eynon E, Brash D, Kashgarian M, Flavell R, Wolin S. A lupus-like syndrome develops in mice lacking the Ro 60-kDa protein, a major lupus autoantigen. Proc Natl Acad Sci USA. 2003; 100:7503–7508. [PubMed: 12788971]
15. Chen X, Wurtmann EJ, Van Batavia J, Zybailov B, Washburn MP, Wolin SL. An ortholog of the Ro autoantigen functions in 23S rRNA maturation in D. radiodurans. Genes Dev. 2007; 21:1328–1339. [PubMed: 17510283]
16. Sim S, Weinberg DE, Fuchs G, Choi K, Chung J, Wolin SL. The subcellular distribution of an RNA quality control protein, the Ro autoantigen, is regulated by noncoding Y RNA binding. Mol Biol Cell. 2009; 20:1555–1564. [PubMed: 19116308]
17. Fouraux MA, Bouvet P, Verkaart S, van Venrooij WJ, Pruijn GJ. Nucleolin associates with a subset of the human Ro ribonucleoprotein complexes. J Mol Biol. 2002; 320:475–488. [PubMed: 12096904]
18. Sim S, Yao J, Weinberg DE, Niessen S, Yates JR 3rd, Wolin SL. The zipcode-binding protein ZBP1 influences the subcellular location of the Ro 60-kDa autoantigen and the noncoding Y3 RNA. RNA. 2012; 18:100–110. [PubMed: 22114317]
19. Clancy RM, Alvarez D, Komissarova E, Barrat FJ, Swartz J, Buyon JP. Ro60-associated single-stranded RNA links inflammation with fetal cardiac fibrosis via ligation of TLRs: a novel pathway to autoimmune-associated heart block. J Immunol. 2010; 184:2148–2155. [PubMed: 20089705]
20. Alvarez D, Briassouli P, Clancy RM, Zavadil J, Reed JH, Abellar RG, Halushka M, Fox-Talbot K, Barrat FJ, Buyon JP. A novel role of endothelin-1 in linking Toll-like receptor 7-mediated inflammation to fibrosis in congenital heart block. J Biol Chem. 2011; 286:30444–30454. [PubMed: 21730058]
21. Maess MB, Sendelbach S, Lorkowski S. Selection of reliable reference genes during THP-1 monocyte differentiation into macrophages. BMC Mol Biol. 2010; 11:90. [PubMed: 21122122]
22. Barrat FJ, Meeker T, Gregorio J, Chan JH, Uematsu S, Akira S, Chang B, Duramad O, Coffman RL. Nucleic acids of mammalian origin can act as endogenous ligands for Toll-like receptors and may promote systemic lupus erythematosus. J Exp Med. 2005; 202:1131–1139. [PubMed: 16230478]
23. Garcia EL, Onafuwa-Nuga A, Sim S, King SR, Wolin SL, Telesnitsky A. Packaging of host mY RNAs by murine leukemia virus may occur early in Y RNA biogenesis. J Virol. 2009; 83:12526–12534. [PubMed: 19776129]
24. Reed JH, Neufing PJ, Jackson MW, Clancy RM, Buyon JP, Gordon TP. Different temporal expression of immunodominant Ro60/60 kDa-SSA and La/SSB apotopes. Clin Exp Immunol. 2007; 148:153–160. [PubMed: 17286801]
25. Reed JH, Giannakopoulos B, Jackson MW, Krilis SA, Gordon TP. Ro60 functions as a receptor for beta2-glycoprotein I on apoptotic cells. Arthritis Rheum. 2009; 60:860–869. [PubMed: 19248095]
26. Reed JH, Clancy RM, Purcell AW, Kim MY, Gordon TP, Buyon JP. {beta}2-Glycoprotein I and Protection from Anti-SSA/Ro60-Associated Cardiac Manifestations of Neonatal Lupus. J Immunol. 2011; 187:520–526. [PubMed: 21602492]
27. Hogg JR, Collins K. Human Y5 RNA specializes a Ro ribonucleoprotein for 5S ribosomal RNA quality control. Genes Dev. 2007; 21:3067–3072. [PubMed: 18056422]
28. Rutjes SA, van der Heijden A, Utz PJ, van Venrooij WJ, Prujin GJM. Rapid nucleolytic degradation of the small cytoplasmic Y RNAs during apoptosis. J Biol Chem. 1999; 274:24799–24807. [PubMed: 10455152]

29. Ayukawa K, Taniguchi S, Masumoto J, Hashimoto S, Sarvotham H, Hara A. La autoantigen is cleaved in the COOH terminus and loses the nuclear localization signal during apoptosis. J Biol Chem. 2000; 275:34465–34470. [PubMed: 10913436]

30. Vollmer J, Tluk S, Schmitz C, Hamm S, Jurk M, Forsbach A, Akira S, Kelly KM, Reeves WH, Bauer S, Krieg AM. Immune stimulation mediated by autoantigen binding sites within small nuclear RNAs involves Toll-like receptors 7 and 8. J Exp Med. 2005; 202:1575–1585. [PubMed: 16330816]

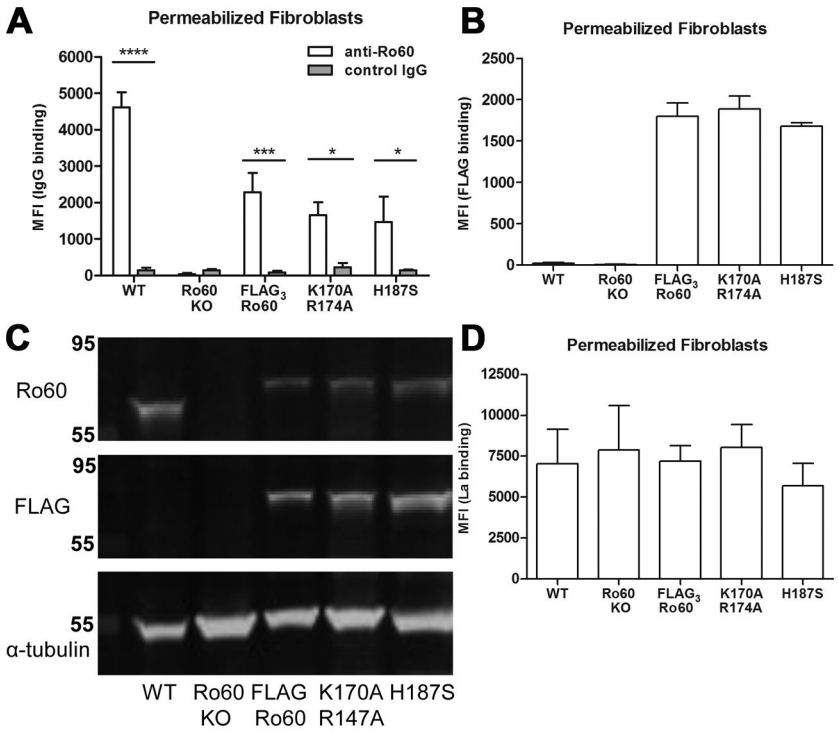

Figure 1.

Intracellular expression of Ro60, FLAG, and La in wild-type (WT), Ro60 knockout (KO), $FLAG_3$-Ro60, $FLAG_3$-Ro60(K170A R174A) and $FLAG_3$-Ro60(H187S) murine fibroblasts. A) Affinity purified human anti-Ro60 Ab (open bars) bound to digitonin-permeabilized fibroblasts expressing WT and mutated forms of Ro60 by flow cytometry. Control IgG purified from a healthy donor (shaded bars) did not bind to permeabilized fibroblasts. Values of mean fluorescence intensity (MFI) are mean ± SEM for 5 experiments. B) Anti-FLAG mAb bound to permeabilized fibroblasts expressing $FLAG_3$-Ro60 constructs by flow cytometry. Values are mean ± SEM for 5 experiments. C) Fibroblasts were lysed, subjected to immunoblot and probed with anti-Ro60 Ab (upper), anti-FLAG mAb (middle) and anti-alpha tubulin mAb (lower). D) Reactivity of affinity purified human anti-La Ab to digitonin-permeabilized murine fibroblasts by flow cytometry. Values are mean ± SEM for 3 experiments. *P<0.05, *** P≤0.0005, ****P≤0.00005.

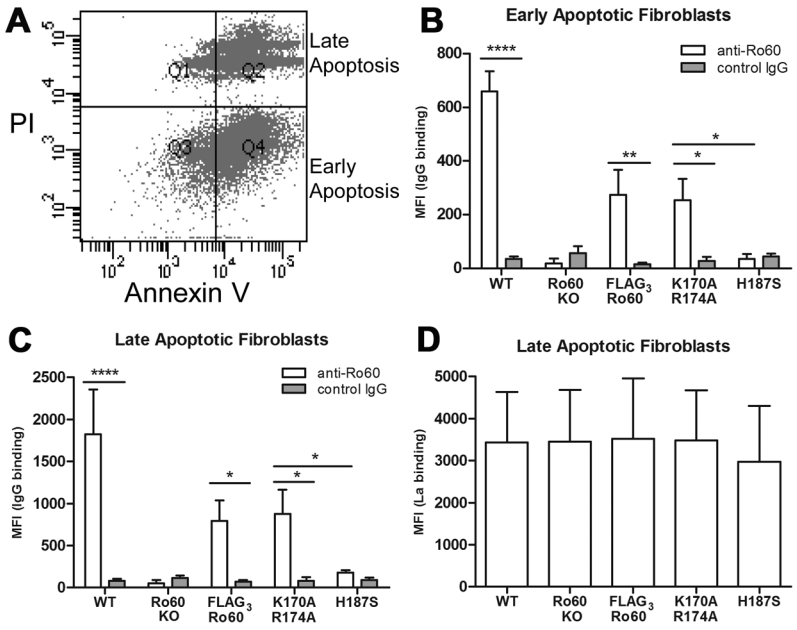

Figure 2.

Cell surface translocation of Ro60 and La on apoptotic fibroblasts; wild-type (WT), Ro60 knockout (KO), $FLAG_3$-Ro60, $FLAG_3$-Ro60 (K170A R174A) and $FLAG_3$-Ro60 (H187S) murine fibroblasts. A) Apoptotic fibroblasts were prepared by plating on poly(2-hydroxyethyl methacrylate) (18 hr, 37°C) and were double stained using annexin V-APC and PI. Representative flow cytometry data highlight early (Quadrant (Q)4, annexin V-positive, PI-negative) and late (Q2, annexin V, PI-positive) cell populations. B) Binding of affinity purified anti-Ro60 Ab to gated early apoptotic fibroblasts. C) Binding of anti-Ro60 Ab to gated late apoptotic fibroblasts. D) Reactivity of affinity purified human anti-La Ab to late apoptotic murine fibroblasts (surface La is not detected on early apoptotic cells (24)). Values are mean ± SEM for 5 experiments. MFI, mean fluorescence intensity. *P<0.05, ** P≤0.005, ****P≤0.00005.

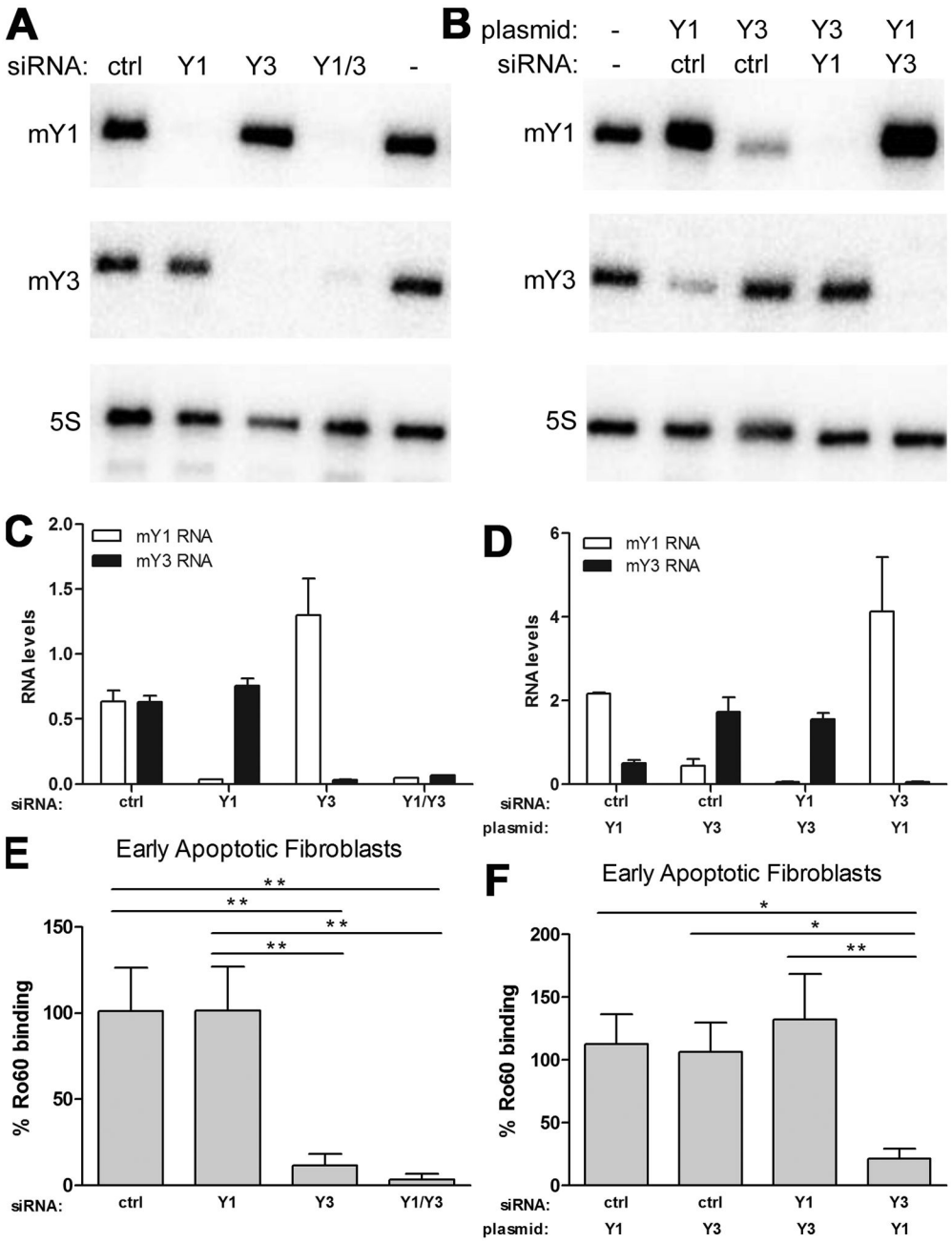

Figure 3.

Cell surface translocation of Ro60 on apoptotic cells is dependent on mY3 RNA. A) Representative northern blot of wild-type fibroblasts subjected to RNA interference with non-targeting control (ctrl), mY1, mY3 or mY1/mY3 small interfering (si) RNA (48 hr, 37°C). B) Northern blot of wild-type fibroblasts co-transfected with siRNA (control, mY1 or mY3) and pBluescriptII KS+ plasmids encoding mY1 or mY3 (48 hr, 37°C). Expression of mY1 (open bars) and mY3 (shaded bars) RNA in wild-type fibroblasts transfected with control, mY1, or mY3 siRNA in the absence (C) or presence (D) of mY1 or mY3 plasmids. E) Flow cytometry analysis of binding of affinity purified anti-Ro60 to early apoptotic fibroblasts transfected with control, mY1, mY3, or mY1/mY3 siRNA relative to untreated

fibroblasts. F) Flow cytometry analysis of binding of affinity purified anti-Ro60 to early apoptotic fibroblasts co-transfected with siRNA and plasmid relative to untreated fibroblasts. Values are mean ± SEM for 4 experiments for C-F. *P<0.05, ** P≤0.005.

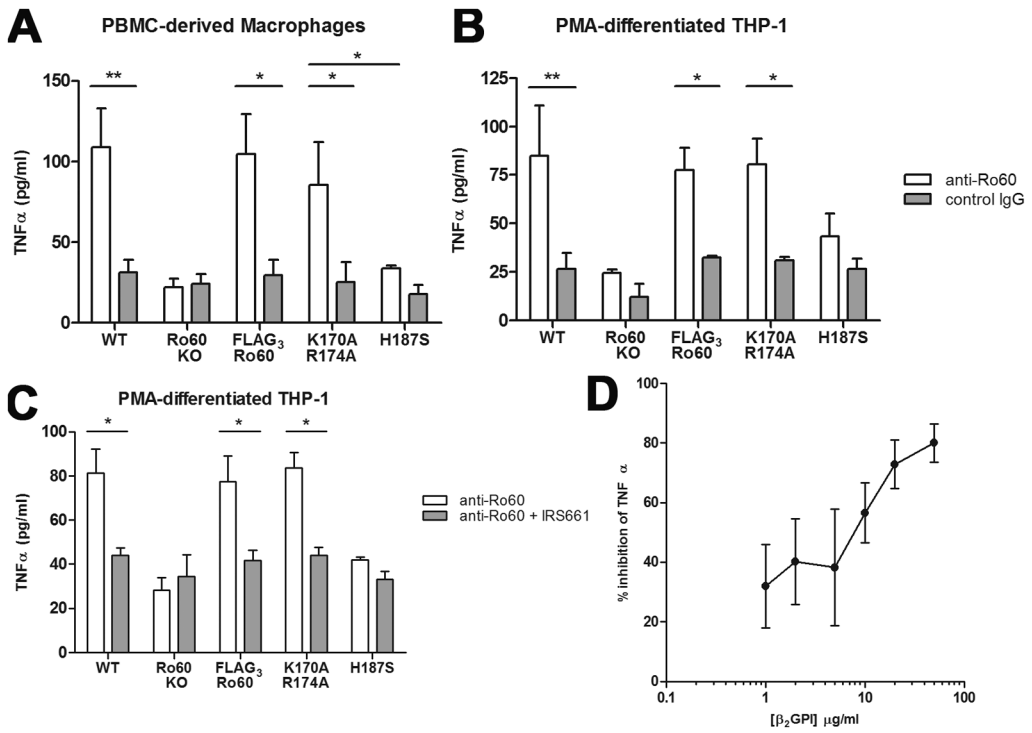

Figure 4.

Apoptotic fibroblast immune complexes containing Y RNA, Ro60 and anti-Ro60 stimulate a TLR7-dependent TNFα secretion by macrophages. PBMC-derived human macrophages (A) and PMA-stimulated THP-1 (B) secreted TNFα when co-cultured with wild-type (WT), $FLAG_3$-Ro60, or $FLAG_3$-Ro60(K170A R174A) apoptotic fibroblasts opsonized with anti-Ro60 (open bars) but not control IgG (shaded bars). Co-cultures with Ro60 knockout (KO) or $FLAG_3$-Ro60(H187S) fibroblasts, preincubated with anti-Ro60 Ab showed lower levels of TNFα that were equivalent to control IgG treatments. C) To support the role of the TLR pathway in macrophage activation, TNFα secretion by THP-1 stimulated by apoptotic fibroblast immune complexes containing Y RNA and anti-Ro60 Ab (open bars) was inhibited by IRS661 (shaded bars), a TLR7 antagonist. Values are mean ± SEM for 5 experiments. D) To support the association of macrophage activation with anti-Ro60 Ab, β_2GPI, previously shown to compete with anti-Ro60 Ab for binding to apoptotic cells, was added to wild-type apoptotic fibroblasts prior to opsonization with anti-Ro60 Ab and co-culture with THP-1. Consistent with the reported interaction of Ro60 and β_2GPI (25, 26); β_2GPI caused a dose-dependent inhibition of TNFα secretion. Values are mean ± SEM for 3 experiments. *$P<0.05$, ** $P\leq0.005$.